



Electronic dynamics under effect of a nonlinear Morse interaction and a static electric field



A. Ranciaro Neto^{a,b}, F.A.B.F. de Moura^{a,*}

^a Instituto de Física, Universidade Federal de Alagoas, Maceió, AL, 57072-970, Brazil

^b Faculdade de Economia, Administração e Contabilidade, Av. Lourival Melo Mota, s/n, bl. 14. Tabuleiro dos Martins 57072-970, Brazil

ARTICLE INFO

Article history:

Received 29 October 2015

Revised 11 April 2016

Accepted 12 April 2016

Available online 20 April 2016

PACS:

63.50.+x

63.22.+m

62.30.+d

Keywords:

Electric field

Soliton

Morse lattice

ABSTRACT

Considering non-interacting electrons in a one-dimension alloy in which atoms are coupled by a Morse potential, we study the system dynamics in the presence of a static electric field. Calculations are performed assuming a quantum mechanical treatment for the electronic transport and a classical Hamiltonian model for the lattice vibrations. We report numerical evidence of the existence of a soliton–electron pair, even when the electric field is turned on, and we offer a description of how the existence of such a phase depends on the magnitude of the electric field and the electron–phonon interaction.

© 2016 Elsevier B.V. All rights reserved.

1. Introduction

The issue concerning the time-dependent behavior of an initially localized electronic wave-packet has a direct connection with the electrical properties of materials [1–6]. The seminal works of Anderson and other co-workers have shown that the presence of disorder is a key factor governing the extension of the wave function [7–10]. They demonstrated that in a disordered system with dimension $d \leq 2$, all eigenstates become localized in a finite fraction of the system, even in the case of weak disorder. The Anderson localization theory has been developed for electrons. However, such a prediction is valid for any field described by a wave equation. Examples for electromagnetic fields [11], water waves [12] and Bose–Einstein Condensates (BEC) [13] have been reported in the literature. Within the context of BEC, we emphasize that its dynamics is well described by the Gross–Pitaevskii equation [14], and the nonlinearity present in this equation reveals exciting new physical properties [15–17].

Nonlinearity can also be found in electronic systems. Some authors [18] have shown that the interaction between electrons and optical phonons is well described by a nonlinear Schrödinger equation. An interesting nonlinear phenomenon, called self trapping (ST), occurs when the nonlinearity strength exceeds the magnitude of the electronic bandwidth [19–26]. When ST takes place, an initially localized wave-packet does not spread over the system, remaining localized around its initial position. In a wider sense, transport properties in nonlinear lattices have attracted a great deal of interest among the solid state community, as well as within the nonlinear science field [27–74]. Davydov [55–59] came up with the idea

* Corresponding author. Tel.: +55 82999593909.

E-mail address: fidelis@fis.ufal.br (F.A.B.F. de Moura).

that the electron–lattice nonlinear term can promote charge transport. That mechanism is a consequence of the nonlinear interaction between a linear electronic model and a linear lattice, whose dynamics are described by a soliton-bearing equation.

Moreover, in [60–71], Velarde and co-workers have shown the existence of a polaron-soliton “quasi-particle” in nonlinear lattices, and also its importance to the charge carry. The coupling of self-trapped states (polaron states) with the lattice solitons has been generally termed as a solectron [60–71]. We highlight that solectron theory represents a generalization of the original polaron concept that is able to mediate non-Ohmic supersonic electric conduction [68]. The electronic transport mediated by nonlinear effects has been investigated in several two-dimensional anharmonic lattices, particularly in a square lattice similar to the cuprate lattice [71]. They found numerical evidence of electron–soliton transfer along the crystallographic axis.

McNeil and co-workers in ref. [75] provided an interesting experimental advance in electron transport. They were able to move a single electron along a wire, batting it back and forth, like the ball in a ping-pong game. The possibility of using this “controlled motion” within the framework of quantum computing, for example, to move a quantum ‘bit’ between two far places, was noted. This experiment consisted of trapping a single electron in a quantum dot and moving this electron around a channel using a surface acoustic wave (SAW). The authors obtained up to 60 shots with a good quality. The possibility of using SAW to move electrons and to construct quantum bits has attracted the attention of the scientific community [76–82].

It is well known that, in the absence of nonlinearity, a static electric field applied parallel to a periodic lattice promotes the dynamic localization of a given initial wave-packet. Furthermore, the presence of a static electric field gives rise to an oscillatory behavior of the electron wave packet (also called “Bloch oscillations”) [83]. The size of the region over which the electron oscillates and the period of these oscillations are inversely proportional to the magnitude of the static electric field. It is worth mentioning that the effect of an electric field in linear chains of molecules was also studied in [84]. These workers considered the Holstein Hamiltonian under the effect of an electric field. Within the Holstein formalism, the lattice is harmonic and the charge becomes trapped due to the presence of a diagonal term related to the lattice oscillations. In particular, they studied the Bloch oscillations of the trapped state and their association with the electron–phonon coupling.

In this work, we push forward the understanding of electronic transport in low-dimensional nonlinear systems under the effect of a uniform electric field. We develop a numerical study of the non-interacting electron dynamics in a one-dimension alloy where the nearest neighbor atoms are coupled by a Morse potential. In addition, we assume a static electric field parallel to the chain. In such a model, the electron transport is treated quantum-mechanically over the alloy in the tight-binding approximation, and the longitudinal vibrations of the lattice are described using a classical formalism. The electron–phonon interaction is introduced by considering electron hopping as a function of the effective distance between neighboring atoms. By solving numerically the dynamic equations for both the electron and the lattice vibrations, we compute the spreading of an initially localized electronic wave-packet. We report numerical evidence of the existence of an electron–soliton pair, even for the presence of a static electric field. We offer a detailed analysis of the dependence of this electron–soliton pair on the magnitude of the electric field and the electron–phonon interaction.

2. Model and numerical calculation

In our work, we consider one electron moving in a 1d anharmonic lattice of N masses under the influence of a static electric field. Our formalism consists of two parts: a quantum Hamiltonian to treat the electron dynamics, and a classical anharmonic Hamiltonian in order to account for the atomic vibrations. The electronic Hamiltonian H_e is defined as [54]:

$$H_e = \sum_n [(n - N/2)eE]D_n^\dagger D_n + \sum_n V_{n+1,n}(D_{n+1}^\dagger D_n). \quad (1)$$

It is a typical one-electron Hamiltonian under the effect of a static electric field E . Here, D_n^\dagger and D_n are the creation and annihilation operators for the electron at site n . eE represents the electric force on the electron of charge e . $(n - N/2)eE$ is the potential energy due to the coupling between the electron and the static electric field E . In order to avoid dealing with large variations in the magnitude of energy along the chain, we shift to zero the potential energy on the center of the lattice by including the constant $-eEN/2$. This is a simple and useful trick that decreases the absolute values of the potential energy, thus improving the numerical stability of our calculations. V_n is the hopping amplitude.

The atomic lattice in our work is defined by a classical Hamiltonian H_{lattice} that considers the nearest neighbor sites coupled by the Morse Potential [52,54]:

$$H_{\text{lattice}} = \sum_n \frac{p_n^2}{2m_n} + C_1 \{1 - \exp[-C_2(q_n - q_{n-1})]\}^2. \quad (2)$$

where p_n and q_n are the momentum and displacement of the mass at site n , respectively. C_1 represents the typical energy of a bond and C_2 is the range parameter of the Morse potential [52,54]. We set $m_n = 1$ and we obtain a dimensionless representation of the quantities q_n , p_n , H by absorbing the constants C_1 and C_2 according to [52,54]: $q_n \rightarrow C_2 q_n$; $p_n \rightarrow p_n/\sqrt{2C_1}$ and $H_{\text{lattice}} \rightarrow H_{\text{lattice}}/(2C_1)$.

Here we follow [52,54] on the interaction between the electron and the vibrational modes. This is considered in our model by relating the electronic parameters $V_{n+1,n}$ to the displacements of the molecular masses from their equilibrium positions. The hopping elements $V_{n+1,n}$ depend on the relative distance between two consecutive molecules of the chain

as: $V_{n+1,n} = -V \exp[-\alpha(q_{n+1} - q_n)]$. The quantity α represents the effective coupling between the relative displacement of lattice units and the hopping term $V_{n+1,n}$, or, in other words, it determines the electron–lattice coupling strength (in units of $1/C_2$). For small displacements, we recover the Su et al. approximation $V_{n+1,n} \approx -V[1 - \alpha(q_{n+1} - q_n)]$ [27].

The time-dependent wave-function $|\Phi(t)\rangle = \sum_n f_n(t)|n\rangle$ is obtained by numerical solution of the time-dependent Schrödinger equation. We consider the electron to be initially localized at site $N/2$, i.e. $|\Phi(t=0)\rangle = \sum_n f_n(t=0)|n\rangle$, where $f_n(t=0) = \delta_{n,N/2}$. The Wannier amplitudes evolve according to the time-dependent Schrödinger equation as ($\hbar = 1$)

$$i \frac{df_n(t)}{dt} = [(n - N/2)F]f_n(t) - \tau \exp[-\alpha(q_{n+1} - q_n)]f_{n+1}(t) - \tau \exp[-\alpha(q_n - q_{n-1})]f_{n-1}(t). \quad (3)$$

The lattice equation can be written as

$$\frac{d^2 q_n(t)}{dt^2} = \{1 - \exp[-(q_{n+1} - q_n)]\} \exp[-(q_{n+1} - q_n)] - \{1 - \exp[-(q_n - q_{n-1})]\} \exp[-(q_n - q_{n-1})] \\ + \alpha V \{ (f_{n+1}^* f_n + f_{n+1} f_n^*) \exp[-\alpha(q_{n+1} - q_n)] - (f_n^* f_{n-1} + f_n f_{n-1}^*) \exp[-\alpha(q_n - q_{n-1})] \} \quad (4)$$

We stress that we used the formalism defined in [52]. Time is scaled as $t \rightarrow \Omega t$ where Ω is the frequency of harmonic oscillations around the minimum of the Morse potential [52]. Here, the generalized hopping $\tau = V/(\hbar\Omega)$ determines the time scale difference between the fast electronic dynamics and the slow lattice vibrations. F is a generalized electric field in dimensionless scale (electric charge, lattice parameter and \hbar are set as unitary).

The equations governing the electron motion (Eq. (3)) are solved numerically by employing a high-order method based on the Taylor expansion of time evolution operator $U(\delta t)$ [73,85]:

$$U(\delta t) = \exp(-i\tilde{H}_e \delta t) = 1 + \sum_{l=1}^{n_0} \frac{(-i\tilde{H}_e \delta t)^l}{l!} \quad (5)$$

where \tilde{H}_e is exactly the same one electron Hamiltonian (Eq. (1)) with normalized hopping $\tilde{V}_{n+1,n} = -\tau \exp[-\alpha(q_{n+1} - q_n)]$. The wave-function at time δt is given by $|\Phi(\delta t)\rangle = U(\delta t)|\Phi(t=0)\rangle$. This method can be used recursively to obtain the wave-function at time t . To obtain $\tilde{H}_e^l |\Phi(t=0)\rangle$, we use a recursive formula derived as follows: let $\tilde{H}_e^l |\Phi(t=0)\rangle = \sum_n Z_n^l |n\rangle$. With the Hamiltonian formula (Eq. (1)) we then compute $\tilde{H}_e^1 |\Phi(t=0)\rangle$ and we have Z_n^1 as

$$Z_n^1 = [(n - N/2)F]f_n(t=0) - \{\tau \exp[-\alpha(q_{n+1} - q_n)]\}f_{n+1}(t=0) - \{\tau \exp[-\alpha(q_n - q_{n-1})]\}f_{n-1}(t=0) \quad (6)$$

Therefore, using $\tilde{H}_e^l |\Phi(t=0)\rangle = \tilde{H}_e \sum_n Z_n^{l-1} |n\rangle$, Z_n^l can be obtained recursively as

$$Z_n^l = [(n - N/2)F]Z_n^{l-1} - \{\tau \exp[-\alpha(q_{n+1} - q_n)]\}Z_{n+1}^{l-1} - \{\tau \exp[-\alpha(q_n - q_{n-1})]\}Z_{n-1}^{l-1}. \quad (7)$$

The classical equations (Eq. (4)) were solved using a second-order Euler method [86]. The procedure starts with a standard Euler method in order to find a prediction $q_n(\delta t)^*$ at the time δt :

$$q_n(\delta t)^* \approx q_n(t=0) + \delta t \left. \frac{dq_n}{dt} \right|_{t=0} \quad (8)$$

The next step consists of applying a correction formula to find a better approximation to $q_n(t + \delta t)$

$$q_n(\delta t) \approx q_n(t=0) + \frac{\delta t}{2} \left[\left. \frac{dq_n}{dt} \right|_{t=0} + \left. \frac{dq_n}{dt} \right|_{\delta t} \right] \quad (9)$$

This method (Eqs. (8) and (9)) can be used recursively to obtain $q_n(t)$. Our main calculations were carried out using $\delta t = 10^{-3}$, and the sum of Eq. (5) was truncated on $n_0 = 15$. Thus, we obtained the wave-function norm with error $|1 - \sum_n |f_n(t)|^2| < 10^{-10}$ along the entire time interval. We emphasize that the norm conservation is a first and important check for the accuracy of our numerical procedure. We also performed a second check using a standard fourth-order Runge-Kutta (RK4) [86] to solve Eqs. (3) and (4). The results obtained using our numerical formalism do not show any difference from those obtained using (RK4).

We recognize that the second-order Euler formalism is not the traditional way to solve the classical equation (Eq. (4)). However, we obtained a negligible difference (less than 10^{-8}) in the atomic position using either RK4 ($\{q_n^{RK4}(t)\}$) or Euler formalism ($\{q_n^E(t)\}$) at the time interval and for the lattice sizes considered here. Also, the Taylor-Euler method requires, on average, one third of the time of the standard RK4 formalism to achieve the same dynamics. It is worth mentioning that a similar numerical formalism was previously used in [87–89]. In these works, a first-order Euler method was employed to solve the lattice equation, and the quantum equation was solved by numerical calculation of the evolution operator [87–89]. However, they used numerical diagonalization of the complete quantum Hamiltonian in order to obtain the evolution operator. In our formalism, the Taylor expansion was used instead, to allow for studying systems with larger sizes in a shorter computational time.

To quantify the electronic transport on this nonlinear model, we computed some typical quantities; namely, the mean position (centroid) and participation function. These are defined as [73,90]

$$\langle n(t) \rangle = \sum_n (n - N/2) |f_n(t)|^2 \quad (10)$$

and

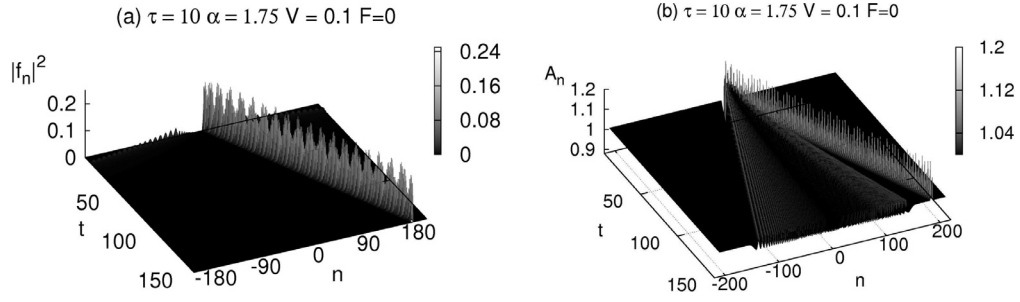


Fig. 1. (a) Squared wave-function component $|f_n|^2$ versus t and n for $\alpha = 1.75, \tau = 10, V = 0.1$ and $F = 0$. (b) Lattice deformation A_n for the same case as in (a).

$$\xi(t) = 1 / \sum_n |f_n(t)|^4. \quad (11)$$

respectively. The centroid for time t represents the mean position of the electron using the center of a self-expanded chain as the origin. The participation function provides an estimate of the number of sites under which the wave-packet is spread at time t .

3. Results and discussions

We considered at $t = 0$ the electron fully localized at the center of a self-expanding chain (i.e. $\{f_n(t=0) = \delta_{n,N/2}\}$). The self-expanding chain was used to minimize border effects; whenever the probability of finding the electron or the atomic vibration at the extremities of the chain exceeded 10^{-30} , 10 new sites were added to each edge. The lattice was initialized using the following initial excitation : $p_n = \delta_{n,N/2}, q_n = 0$. Numerical convergence of our calculations was ensured by checking the conservation of the norm of the wave-packet at every time step; our results provide $|1 - \sum_n |f_n(t)|^2| < 10^{-10}$ for all times considered. At first, we analyzed exactly the same case presented in [52]: $\tau = 10, \alpha = 1.75, V = 0.1$ and $F = 0$, because we want to bring the reader's attention to the electron–soliton pair formation, and because it is an additional way to validate our numerical formalism. We reiterate that the presence of the electric field and its competition with the nonlinear lattice vibration are the main focus of our work. The case without an electric field ($F = 0$) was investigated in [52].

In Fig. 1(a) we plot the electronic wave-function at the $n \times t \times |f_n|^2$ plane, while in (b) we show the lattice deformation in the $n \times t \times A_n$ plane for the absence of electric field ($F = 0$), where $A_n = \exp[-(q_n - q_{n-1})]$. For those three-dimensional graphics, $n = 0$ represents the center of the self-expanded chain.

We observe that the wave-function remains trapped in a finite fraction of lattice. In addition, we notice that the localized electronic wave-packet moves along the chain. We also see that there are some tiny spikes that deviate from the center of the chain with a fraction of the wave-packet that remains trapped and moving along the chain. These spikes represent a tiny fraction of the wave-packet that escapes and spreads freely along the nonlinear chain. Similar phenomena are present in the works of Velarde [50–53].

The results for the deformation A_n reveal that the initial energy propagates along the classical chain in a solitonic state. Our calculations for $F = 0$ are in agreement with the previous calculations of [52], where this kind of electron–soliton pair was reported for the first time. After having revisited the phenomenology of the electronic dynamics under the effect of nonlinear lattice vibration, we considered the electric field term. As mentioned previously, the calculations for $F > 0$ and their consequences on the electron–lattice dynamics represent the main novelty of our work.

The effect of the electric field is considered initially by analyzing the same case as in Fig. 1 for $F > 0$. Based on the topological profile of the previous case for $F = 0$, we notice that the electronic mean position increases with time, and the participation number remains constant. We investigate the effect of electric field on those functions for the same set of parameters considered in Fig. 1. In Fig. 2(a) we show the long-time behavior of the mean position, computed as the average of $\langle n(t) \rangle$ in the long time limit $\langle n \rangle = (\sum_{t=0.8t_{max}}^{t_{max}} \langle n(t) \rangle) / N_{times}$ (here $t_{max} = 2 \times 10^3$), versus the magnitude of the electric field F . For the electric field within the interval $(0 < F < 2)$, we observe that $\langle n \rangle$ is large, thus suggesting that the electron still moves along the chain. However, outside this interval, the electron remains trapped around the initial position. We emphasize here that there is an intricate phenomenology behind these results. Formally, when a static electric field is applied parallel to the chain, the electron should remain trapped around the initial position, performing an oscillatory behavior with a frequency equal to the magnitude of the electric field (i.e. Bloch-oscillation). In our case, we observe that the competition between the static electric field and the electron–soliton term seems to break down the Bloch-oscillations. For $F > 2$ the electron becomes trapped around the initial position, even in the presence of the electron–soliton term.

Fig. 2(b) shows the long-time mean participation number $\langle \xi \rangle = (\sum_{t=0.8t_{max}}^{t_{max}} \langle \xi(t) \rangle) / N_{times}$ versus the electric field F . We observe that, for all electric field values considered, the participation number is small, thus signaling the trapped character of the electron wave-packet. We will return to discuss particularly the behavior of the participation number later.

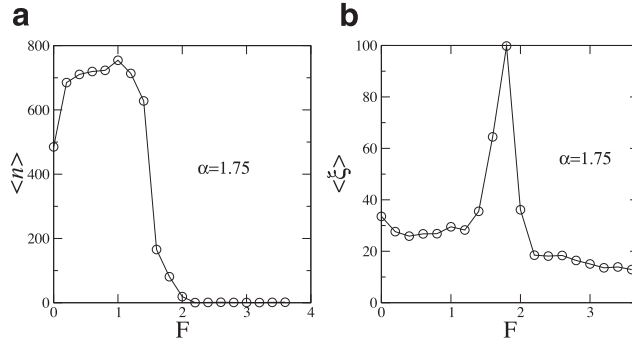


Fig. 2. (a) Electron mean position (centroid) (a) and participation number (b) after a long propagation time versus the electric field magnitude F .

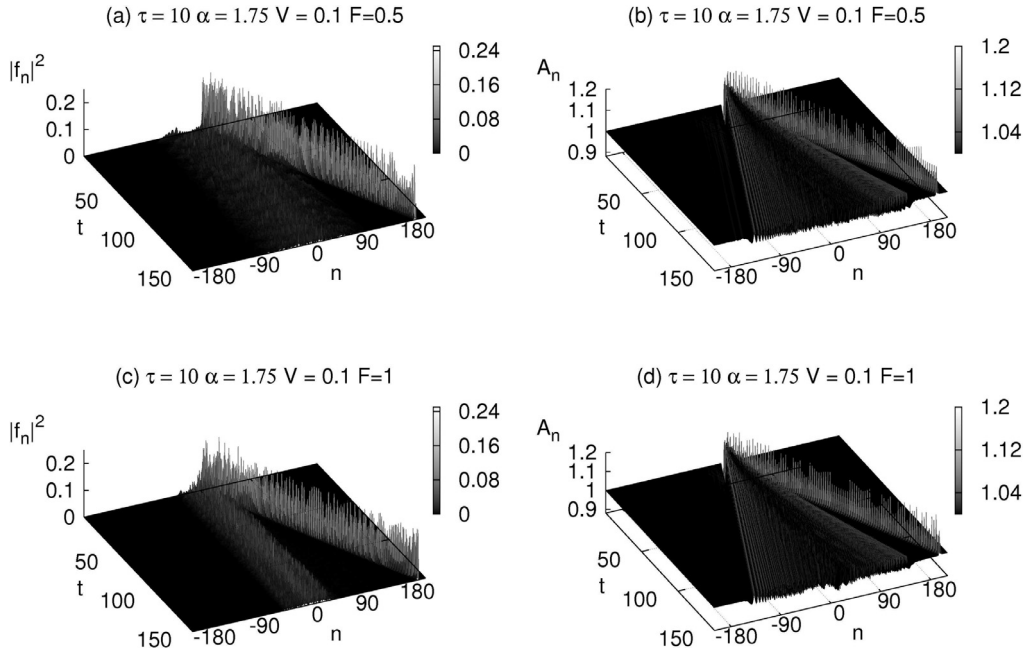


Fig. 3. (a,c) Squared wave-function component $|f_n|^2$ versus t and n for $\alpha = 1.75, \tau = 10, V = 0.1$ and $F = 0.5, 1$. (b,d) Lattice deformation A_n for the same cases respectively in (a,c).

For now, we comment that for $F \leq 2$, the electron is trapped by the solitonic modes that exist within the chain. For $F > 2$, the electric field effect is dominant and keeps the electron trapped around the initial position. For the electric field within the interval ($1.5 < F < 2$) we found a crossover region in which a finite fraction of the wave-function remains trapped around the initial position, and another small part participates in the electron–soliton dynamics. This crossover effect increases the participation number (as we can observe for example in Fig. 2(b) for $F \approx 1.8$). We obtain a major understanding of the electronic behavior for ($F \leq 2$) by analyzing the wave-packet profile and lattice deformation.

For $\tau = 10$, $\alpha = 1.75$ and $V = 0.1$ (i.e. the same as in Fig. 1) and $F \neq 0$, the results of wave-packet and the lattice deformation are reported in Figs. 3 and 4. We observe in Fig. 3 for $F = 0.5, 1$ that the wave-function splits into two parts: one moves along the chain and the other (the smallest part) remains trapped around the initial position. Therefore, for a weak electric field, the solitonic mode can still trap a finite fraction of the wave-packet and drag it along the chain. We also observe that the lattice deformation A_n still exhibits a solitonic behavior. We mention that for $F > 0$, the lattice deformations A_n is minimally modified due to the last term of Eq. (4). This term represents an effective force related to the electronic wave-function. Due to the presence of an electric field, this effective force also depends on the electric field, and thus promotes some small differences in the distribution of lattice deformations.

In Fig. 4 we plot our results for $F = 1.8$ and 2. For $F = 1.8$, most of the wave-function remains trapped around the initial position. However, a small part of the initial wave-packet seems to still be captured by the solitonic modes. The configuration found for $1.5 < F < 2$ is distinct from the behavior for $F = 0.5, 1$. (see Fig. 3) where the major part of the wave-packet remains trapped by the solitonic mode. This is the key ingredient behind the increment in the participation number for $F = 1.8$ (see Fig. 2(b)). Our results suggest that for $F \lesssim 1.5$, it is possible that an electron–soliton pair exists due

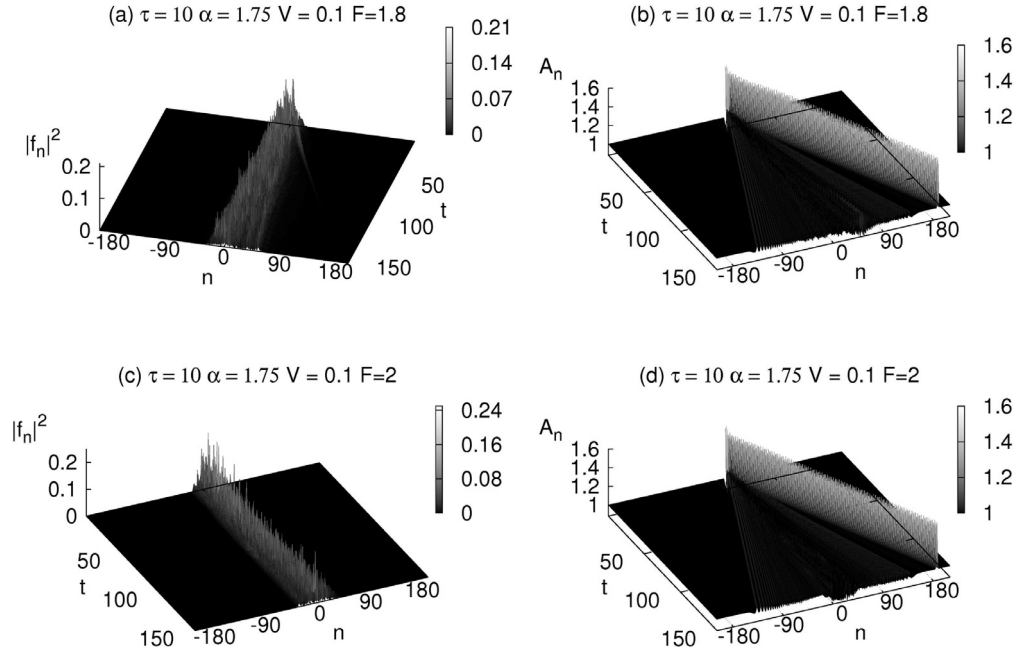


Fig. 4. (a,c) Squared wave-function component $|f_n|^2$ versus t and n for $\alpha = 1.75, \tau = 10, V = 0.1$ and $F = 1.8, 2$. (b,d) Lattice deformation A_n for the same cases respectively in (a,c).

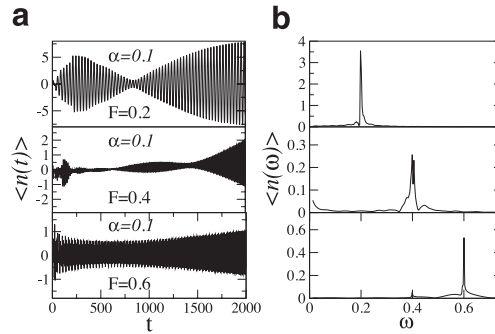


Fig. 5. Left panel: the electron centroid for $\alpha = 0.1$ and $F = 0.2, 0.4, 0.6$. Right panel: The Fourier transform $\langle n(\omega) \rangle$ of the centroid for the same cases showed in the left panel. We observe that for all electric fields considered, the electron position exhibits a Bloch-like oscillatory behavior with frequency ($\omega \approx F$).

to the Morse interaction and the electron–phonon coupling. For $F > 2$, the electron becomes localized around the initial position for this degree of electron–phonon coupling. We emphasize that the electron–phonon term $\alpha = 1.75$ considered in the previous results corresponds to a strong electron–lattice interaction as mentioned in [52]. Moreover, this value is quite close to the higher values of α that we have considered. Further analysis on electron–phonon interaction values can be found later. The region with $1.5 < F < 2$ represents an anomalous crossover region in which the electron–phonon term is insufficient to promote the capture of the electron by the solitonic mode, leaving the largest fraction of the wave-packet around the lattice center.

The main conclusion of the previous figures is that, within the framework of a single electron subjected to a static electric field and the electron–phonon coupling, the interaction with the nonlinear lattice vibrations plays a predominant role. We analyze in more detail this competition between the electric field and the electron–phonon coupling now. For example, in Fig. 5(a) we plot the electron position for $\alpha = 0.1$ and $F = 0.2, 0.4, 0.6$. We notice that, for all electric fields considered, the electron exhibits an oscillatory behavior quite compatible with the well-known Bloch oscillation phenomenon. In Fig. 5(b), we plot the Fourier transform $\langle n(\omega) \rangle$ of the mean centroid in case (a). The main frequency value is around the electric field magnitude ($\omega \approx F$), which is in good agreement with the semi-classical approach. This is a clear signature that, for a weak electron–phonon interaction, the electric field traps the electron wave-function and promotes a quasi-coherent Bloch-like oscillatory motion. We stress that the oscillatory behavior obtained here is slightly different to the standard Bloch-oscillation [83]. In our model, electronic hopping, even for weak electron–phonon coupling, changes along the chain, thus promoting a weak absence of periodicity that can “destroy” the Bloch oscillations for sufficient long times.

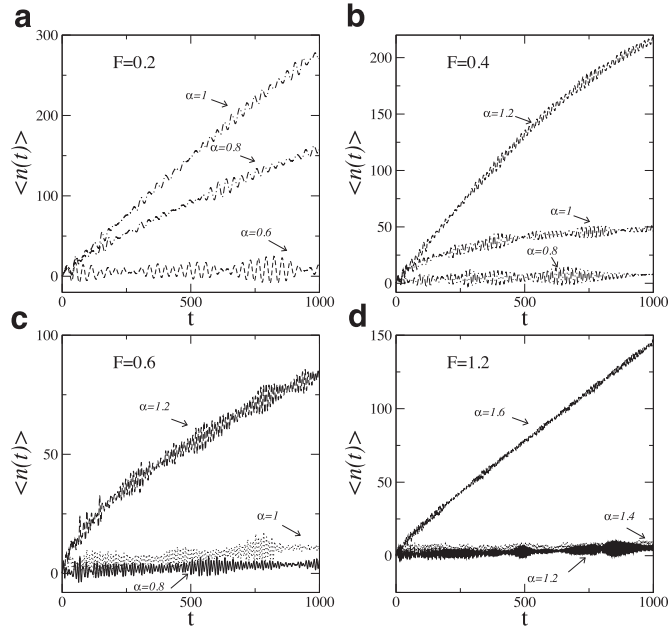


Fig. 6. Electronic centroid $\langle n(t) \rangle$ versus time for $F = 0.2, 0.4, 0.6, 1.2$ and several values of the electron–phonon coupling α . We observe that for each electric field considered there is a specific value of α that separates the phase in which the electron exhibits a Bloch-like oscillation behavior and the phase with the electron–soliton pair formation.

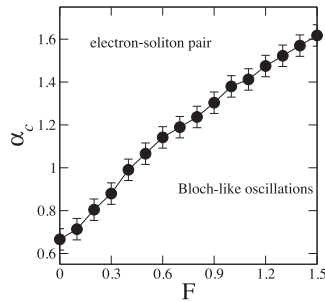


Fig. 7. Phase diagram $\alpha_c \times F$ in order to characterize the (Bloch-like oscillation)/(electron–soliton pair) transition.

However, even considering such possible coherence loss, the electronic localized state exhibits quasi-coherent dynamics with a dominant frequency $\omega \approx F$. Now, we analyze the electron–phonon threshold necessary for the electron–soliton pair formation. In Fig. 6(a–d) we plot the electronic centroid $\langle n(t) \rangle$ versus time for $F = 0.2, 0.4, 0.6, 1.2$ and several values of electron–phonon coupling α . We observe that the electron–lattice interaction α changes the electronic dynamics dramatically. In general, for weak α , we found a localized wave–packet behavior, while the electron moves along the chain for strong α . Therefore, our results suggest that α promotes a transition from a localized state to an electron–soliton pair formation.

We provide in Fig. 7 a phase diagram $\alpha_c \times F$ in order to characterize the (Bloch-like oscillation)/(electron–soliton pair) transition. Fig. 7 was constructed by monitoring the behavior of $\langle n(t) \rangle$ and $\xi(t)$ for each value of F and α . The Bloch-like oscillation phase is described by an oscillatory behavior of $\langle n(t) \rangle$ with dominant frequency $\omega \approx F$. Moreover, the participation number is also small due to the localization process imposed by the electric field. The phase with electron–soliton pair formation is mainly characterized by the absence of coherent oscillations and by the continuous increase of the mean position. The electronic mean position is similar to the average position of the lattice deformation, and propagates roughly with the same velocity. The participation number within this phase also saturates in a small value, thus suggesting that the electron is trapped by the soliton. We monitor the value of α necessary to promote the crossover between these two regimes. The critical point was obtained as $\alpha_c = \langle \alpha_c \rangle \pm \Delta\alpha_c$, with tolerance $\Delta\alpha_c \approx 0.05$. For $\alpha > \alpha_c$, we have the phase with electron–soliton pair and for $\alpha < \alpha_c$ we have the phase with Bloch-like oscillations. For α values within the interval $[\langle \alpha_c \rangle - \Delta\alpha_c, \langle \alpha_c \rangle + \Delta\alpha_c]$ we found a crossover region between both phases.

We also observe that, even in the absence of an electric field ($F = 0$), there is a minimum value of the nonlinearity ($\alpha_c \approx 0.65 \pm 0.05$) necessary to bind the electron to the solitonic mode of the chain. Although the case with $F = 0$ was investigated in [52], the critical value of the electron–lattice interaction necessary to promote the electron–soliton pair has not been hitherto reported. In the absence of an electric field and small α ($\alpha < \alpha_c$) the electronic dynamics exhibits an

interesting behavior: a large fraction of the wave-packet remains free to move along the chain, and a tiny fraction of the wave-packet is trapped by the solitonic mode. Therefore, for weak electron–phonon coupling, the solitonic mode is unable to capture the electron efficiently and drive it at the same soliton velocity. We also observe in Fig. 7 that, as the electric field value F is increased, the critical electron–phonon value α_c also increases. For $F \neq 0$, dynamic localization in general takes place. The interaction of the electron with the static electric field promotes the appearance of a linear potential energy that traps the electron around the initial position and induces Bloch-like oscillations. As the electric field increases, it becomes more difficult for the electron–phonon term to capture a large fraction of the electron wave; thus α_c should increase also (as observed in Fig. 7).

For $F > 2$, the electron becomes roughly trapped and the electron–phonon coupling, within our numerical accuracy, cannot promote the pair formation. For the electric field within the interval ($1.5 < F < 2$), as was described previously, we found a crossover region in which a larger fraction of the wave-function remains trapped around the initial position, and a smaller part joins the electron–soliton dynamics. In our calculations, we found good accuracy until $\alpha \approx 2$. Perhaps for electron-phonon couplings larger than $\alpha = 2$, electron-soliton pair formation could happen also for $F > 1.5$. However, it is difficult to solve the set of quantum/classical equations for large electric fields and electron-phonon interaction. We tried to solve the model at this limit ($1.5 < F < 2$ and $\alpha > 2$) using another high-order integrator (the fourth- (RK4) and also eighth- (RK8) order Runge–Kutta methods). Even with those high-order methods, we did not find sufficient accuracy to perform a definitive analysis. In [51,53,53], the limit $\alpha > 2$ was also avoided.

4. Conclusions

In this work, we studied one-electron dynamics in a one-dimensional Morse model considering a static electric field applied parallel to the chain. Also, we assumed the electron to be described by a quantum-mechanical formalism, while the longitudinal vibrations of the lattice are treated classically. The electron-phonon interaction was introduced by considering the hopping between neighboring sites to be dependent on their relative distance.

By solving numerically the equations for the electron and lattice, we have computed the dynamics of an initially localized electronic wave-packet. Our results can be summarized as follows: for a weak electric field, our calculations have revealed evidence of electron-soliton pair formation. We also found, by numerical means, that the electron-phonon coupling dominates the dynamics, thus destroying the Bloch-oscillation phenomenon. For strong electric fields, the wave-packet remains trapped around the initial position. The solitonic lattice deformations exhibit small losses and remain trapped due to the electric field competitive effect.

We also analyzed in more detail the competitive process between the electric field and the electron-phonon coupling by examining the critical value of the electron-phonon interaction necessary to promote the electron-soliton pair formation under the effect of a static electric field. By monitoring the electronic dynamics for a range of F and α values, we provided a phase diagram in order to characterize the transition between both phases (viz. Bloch-like oscillation/electron-soliton pair). We found the critical electron-phonon interaction necessary to promote the damping of the Bloch-oscillatory behavior and to stabilize a mobile electron-soliton pair. We hope that our work motivates additional investigation within the problem of electronic dynamics under the effect of an electric field and electron-phonon term. There are some interesting and challenging related questions, such as the role played by the electron–electron interaction and by lattice topology.

Acknowledgments

This work was partially supported by CNPq, CAPES, and FINEP (Federal Brazilian Agencies), CNPq-Rede Nanobioestruturas, as well as FAPEAL (Alagoas State Agency). We are grateful to Profs. Drs. M.L. Lyra and M.G. Velarde for useful discussions, corrections and suggestions.

References

- [1] Cheni D, Molina MI, Tsironis GP. *J Phys Cond Matter* 1993;5:8689.
- [2] Silva AFG, Lima RPA, Chaves V, de Moura FABF, Lyra ML. *Commun Nonlinear Sci Numer Simulat* 2016;30:101.
- [3] Longhi S. *J Phys Condens Matter* 2014;26:255504.
- [4] Longhi S. *J Phys Condens Matter* 2012;24:435601.
- [5] Longhi S, Szameit A. *J Phys Condens Matter* 2013;25:035603.
- [6] Kramer B, MacKinnon A. *Rep Prog Phys* 1993;56:1469; Ziman TAL. *Phys Rev Lett* 1982;49:337.
- [7] Abrahams E, Anderson PW, Licciardello DC, Ramakrishnan TV. *Phys Rev Lett* 1979;42:673.
- [8] Anderson PW. *Phys Rev* 1958;109:1492.
- [9] Anderson PW. *Science* 1972;177:393–6.
- [10] Anderson PW. *Philos Mag B*. 1985;52:505–9.
- [11] Wiersma DS, Paolo Bartolini, Ad Lagendijk and Roberto Righini, *Nature* 1997;390:671.
- [12] Billy J. *Nature* 2008;453:891.
- [13] Roati G. *Nature* 2008;453:895.
- [14] Dalfovo F, Giorgini S, Pitaevskii LP, Stringari S. *Rev Mod Phys* 1999;71:463.
- [15] Ryu C, Andersen MF, Vaziri A, dArcy MB, Gross-man JM, Helmerson K, et al. *Phys Rev Lett* 2006;96:160403.
- [16] Behinaein G, Ramareddy V, Ahmadi P, Summy GS. *Phys Rev Lett* 2006;97:244101.
- [17] Johansson M, Hörnquist M, Riklund R. *Phys Rev B* 1995;52:231.
- [18] Datta PK, Kundu K. *Phys Rev B* 1996;53:14929.
- [19] Kopidakis G, Komineas S, Flach S, Aubry S. *Phys Rev Lett* 2008;100:084103.

- [20] Skokos C, Krimer DO, Komineas S, Flach S. Phys Rev E 2009;79:056211. Rev. E 89, (2014) 029907.
- [21] Pan Z, Xiong S, Gong C. Phys Rev E 1997;56:4744.
- [22] de Moura FABF, Gléria I, dos Santos IF, Lyra ML. Phys Rev Lett 2009;103:096401.
- [23] Iomin A. Phys Rev. E 2010;81:017601.
- [24] Caetano RA, de Moura FABF, Lyra ML. Eur Phys J B 2011;80:321.
- [25] Tietsche S, Pikovsky A. Europhys Lett 2008;84:10006.
- [26] Dias WS, Lyra ML, de Moura FABF. Eur Phys J B 2012;85:7.
- [27] Su WP, Schrieffer JR, Heeger AJ. Phys Rev Lett 1979;42:1698.
- [28] Skokos C, Flach S. Phys Rev E 2010;82:016208.
- [29] Ivanchenko MV, Laptyeva TV, Flach S. Phys Rev Lett 2011;107:240602.
- [30] Skokos C, Gkolias I, Flach S. Phys Rev Lett 2013;111:064101.
- [31] Bodyfelt JD, Laptyeva TV, Gligoric G, Krimer DO, Skokos C, Flach S. Int J Bifurc Chaos 2011;21:2107–24.
- [32] Flach S. Nonlinear Dynamics: Materials, Theory and Experiments. Springer Proceedings in Physics 2016;173:45.
- [33] Laptyeva TV. J Phys A 2014;47:493001.
- [34] Pikovsky A. J Stat Mech Theory Exp 2015:P08007.
- [35] de Moura FABF, Gléria I, dos Santos IF, Lyra ML. Phys Rev Lett 2009;103:096401.
- [36] de Moura FABF, Vidal EJGG, Gleria I, Lyra ML. Phys Lett A 2010;374:4152.
- [37] de Moura FABF, Caetano RA, Santos B. J Phys: Condens Matter 2012;24:245401.
- [38] Pan Z, Xiong S, Gong C. Phys Rev E 1997;56:4744; Yamada H, Iguchi K. Adv Cond Mat Phys 2010;2010:380710.
- [39] Kopidakis G, Komineas S, Flach S, Aubry S. Phys Rev Lett 2008;100:084103; Pikovsky AS, Shepelyansky DL. Phys Rev Lett 2008;100:094101; Hajnal D, Schilling R. Phys Rev Lett 2008;101:124101; Lahini Y, Avidan A, Pozzi F, Sorel M, Morandotti R, Christodoulides DN. Phys Rev Lett 2008;100:013906.
- [40] Skokos C, Krimer DO, Komineas S, Flach S. Phys Rev E 2009;79:056211; Skokos C, Krimer DO, Komineas S, Flach S. Phys Rev E 2014;89:029907.
- [41] Leykam D, Flach S, Bahat-Treidel O, Desyatnikov AS. Phys Rev B 2013;88:224203; Gligoric G, Rayanov K, Flach S. EPL 2013;101:10011.
- [42] Laptyeva TV, Bodyfelt JD, Flach S. EPL 2012;98:60002; Larcher M, Laptyeva TV, Bodyfelt JD, Dalfovo F, Modugno M, Flach S. New J Phys 2012;14:103036.
- [43] Xue J-K, Zhang A-X. Phys Rev Lett 2008;101:180401; Akhmediev N, Ankiewicz A, Soto-Crespo JM. Phys Rev E 2009;80:026601; Ponomarenko SA, Agrawal GP. Phys Rev Lett 2006;97:013901; Maluckov A, Hadzievski Lj, Lazarides N, Tsironis GP. Phys Rev E 2009;79:025601(R); Lahini Y, Avidan A, Pozzi F, Sorel M, Morandotti R, Christodoulides DN. Phys Rev Lett 2008;100:013906; Anker Th, Albiez M, Gati R, Hunsmann S, Eiermann B, Trombettoni A. Phys Rev Lett 2005;94:020403.
- [44] Su WP, Schrieffer JR, Heeger AJ. Phys Rev Lett 1979;42:1698; Su WP, Schrieffer JR, Heeger AJ. Phys Rev B 1980;22:2099; Heeger AJ, Kivelson S, Schrieffer JR, Su W-P. Reviews of Modern Physics 1988;60:781.
- [45] Pan Z, Xiong S, Gong C. Phys Rev B 1997;56:1063.
- [46] Macías-Díaz JE, Medina-Ramírez IE. Commun Nonlinear Sci Numer Simul 2009;14:3200.
- [47] Zabusky NJ. Chaos 2005;15:015102.
- [48] Dauxois T, Peyrard M, Ruffo S. Eur J Phys 2005;26:S3–S11.
- [49] Brizhik L, Chetverikov AP, Ebeling W, Röpke G, Velarde MG. Phys Rev B 2012;85:245105.
- [50] Chetverikov AP, Ebeling W, Velarde MG. Physica D 2011;240:1954.
- [51] Hennig D, Velarde MG, Ebeling W, Chetverikov AP. Phys Rev E 2008;78:066606.
- [52] Hennig D, Chetverikov A, Velarde MG, Ebeling W. Phys Rev E 2007;76:046602.
- [53] Makarov V, Velarde MG, Chetverikov AP, Ebeling W. Phys Rev E 2006;73:066626.
- [54] Hennig D, Neissner C, Velarde MG, Ebeling W. Phys Rev B 2006;73:024306.
- [55] Davydov AS. Solitons in Molecular Systems. 2nd ed. Reidel, Dordrecht; 1991.
- [56] Scott AC. Phys Rep 1992;217:1–67.
- [57] Davydov AS. Physica Scripta 1979;20:387–94.
- [58] Davydov AS. J Theor Biol 1977;66:379–87.
- [59] Davydov AS. Biology and quantum mechanics. Pergamon, New York; 1982.
- [60] Alder BJ, Runge KJ, Scalettar RT. Phys Rev Lett 1997;79:3022.
- [61] Brizhik LS, Eremko AA. Physica D 1995;81:295–304.
- [62] Ross OGC, Cruzeiro L, Velarde MG, Ebeling W. Eur Phys J B 2011;80:545–54.
- [63] Velarde MG, Neissner C. Int J Bifurc Chaos 2008;18:885–90.
- [64] Velarde MG, Ebeling W, Chetverikov AP. Int J Bifurc Chaos 2011;21:1595–600.
- [65] Chetverikov AP, Ebeling W, Velarde MG. Eur Phys J B 2011;80:137–45.
- [66] Hennig D, Velarde MG, Ebeling W, Chetverikov A. Phys Rev E 2007;78:066606.
- [67] Velarde MG, Ebeling W, Chetverikov AP. Internat J Bifurc Chaos 2005;15:245.
- [68] Velarde MG. J Comput Appl Math 2010;233:1432.
- [69] Velarde MG, Ebeling W, Chetverikov AP. Eur Phys J B 2012;85:291.
- [70] Ebeling W, Chetverikov AP, Röpke G, Velarde MG. Contrib Plasma Phys 2013;53:736.
- [71] Chetverikov AP, Ebeling W, Velarde MG. Eur Phys J Spec Topics 2013;222:2531.
- [72] Velarde MG, Chetverikov, Chetverikov AP, Ebeling W, Wilson EG, Donovan KJ. EPL 2014;168:27004.
- [73] Sales MO, de Moura FABF. J Phys Condens Matter 2014;26:415401.
- [74] Sales MO, Fulco UL, Lyra ML, Albuquerque EL, de Moura FABF. J Phys Condens Matter 2015;27:035104.
- [75] McNeil RPG, Kataoka M, Ford CJB, Barnes CHW, Anderson D, Jones GAC, et al. Nature 2011;477:439–42.
- [76] Barnes CHW, Shilton JM, Robinson AM. Phys Rev B 2000;62:8410.
- [77] Astley MR, Kataoka M, Ford CJB, Barnes CHW, Anderson D, Jones GAC, et al. Phys Rev Lett 2007;99:156802.
- [78] Sanada H, Sogawa T, Gotoh H, Onomitsu K, Kohda M, Nitta J, et al. Phys Rev Lett 2011;106:216602.
- [79] Astley MR, Kataoka M, Ford CJB, Barnes CHW, Anderson D, Jones GAC, et al. Physica E 2008;40:1136.
- [80] Volk S, Schülein FJR, Knall F, Reuter D, Wiecek AD, Truong TA, et al. Nano Lett 2010;10:3399.
- [81] Schülein FJR, Müller K, Bichler M, Koblmüller G, Finley JJ, Wixforth A, et al. Phys Rev B 2013;88:085307.
- [82] Neto AR, Sales MO, de Moura FABF. Solid State Commun 2016;229:22.
- [83] Domínguez-Adame F, Malyshev VA, de Moura FABF, Lyra ML. Phys Rev Lett 2003;91:197402.
- [84] Lakhnoa VD, Korshunova AN. Eur Phys J B 2007;55:85.
- [85] de Moura FABF. Int J M Phys C 2011;22:63.
- [86] Hairer E, Nørsett SP, Wanner G. Solving Ordinary Differential Equations I: Nonstiff Problems. 3rd ed. New York: (Springer Series in Computational Mathematics); 2007; Press WH, Flannery WP, Teukolsky SA, Wetterling WT. Numerical Recipes: The Art of Scientific Computing. 3rd ed. New York: Cambridge University Press; 2007.
- [87] Lima MP, Silva GMe. Phys Rev B 2006;74:224304.
- [88] Silva GMe, de Brito AN, Correia N. Phys Rev B 1996;53:7222.
- [89] Ribeiro LA Jr, Cunha WFd, Fonseca ALA, Silva GMe, Stafström S. J Phys Chem Lett 2015;6:510.
- [90] dos Santos JLL, Nguyen BP, de Moura FABF. Physica A 2015;435:15–21.